

Ab initio charge, spin and orbital energy scales in  $\text{LaMnO}_3$ R. T. Yier<sup>1,2</sup>, W. M. Temmerman<sup>1</sup>, Z. Szotek<sup>1</sup>, G. Banach<sup>1</sup>, A. Svane<sup>3</sup>, L. Petit<sup>3</sup>, G. A. Gehring<sup>2</sup><sup>1</sup> Daresbury Laboratory, Daresbury, Warrington WA4 4AD, UK<sup>2</sup> Department of Physics and Astronomy, University of Sheffield, Sheffield, S3 7RH, UK and<sup>3</sup> Department of Physics and Astronomy, University of Aarhus, DK-8000 Aarhus, Denmark  
(Dated: March 22, 2024)

The first-principles SIC-LSD theory is utilized to study electronic, magnetic and orbital phenomena in  $\text{LaMnO}_3$ . The correct ground state is found, which is antiferro orbitally ordered with the spin magnetic moments antiferromagnetically aligned. Jahn-Teller energies are found to be the largest energy scale. In addition it is the Jahn-Teller interaction which is the dominant effect in realising orbital order, and the electronic effects alone do not suffice.

PACS numbers: PACS 71.27.+a, 71.28.+d

There are several transition metal compounds in which the orbital degeneracy is broken spontaneously. Examples are  $\text{KCuF}_3$ , [1]  $\text{V}_2\text{O}_3$ , [2] and the manganites, [3] which are the subject of the present study. In the manganites, the crystal field associated with  $\text{MnO}_6$  octahedra splits the manganese d levels into a lower lying  $t_{2g}$  triplet and an upper  $e_g$  doublet. The  $t_{2g}$  states are highly localized whereas an electron in one of the  $e_g$  states is potentially itinerant. The  $\text{Mn}^{4+}$  ion in  $\text{CaMnO}_3$  has a fully occupied majority  $t_{2g}$  manifold and empty  $e_g$  states, which form a strongly localized core spin  $S = \frac{3}{2}$ . The  $\text{Mn}^{3+}$  ion in  $\text{LaMnO}_3$ , on the other hand, has an additional d electron which, due to the strong intra-atomic exchange, populates one of the  $e_g$  states, forming an  $S = 2$  spin, and which gives rise to a Jahn-Teller (JT) instability. In this system each of the oxygen ions is a neighbour to two Mn ions and hence the local distortions of the lattice must be arranged in such a way as to minimize the energy for the whole crystal. This gives rise to Mn-O bond lengths of 1.90 and 2.18 Å within the manganese oxygen plane, compared with 1.96 Å for the hypothetical cubic system. The  $e_g$  states rotate to form an orbitally ordered lattice of  $d_{3x^2-r^2}$  and  $d_{3y^2-r^2}$  orbitals in the manganese oxygen plane [4], shown schematically in Fig. 1.

This paper reports a first-principles study of charge, spin and orbital energy scales in  $\text{LaMnO}_3$ , with the emphasis on orbital ordering (OO), based upon the self-interaction corrected (SIC) local spin-density (LSD) theory, [5, 6] which allow s-d electron localization to be distinguished from itinerancy, in an ab initio manner. [7, 8] Not only does the SIC allow the localization of an orbital of any symmetry, but the SIC-LSD total energies can be minimized with respect to the number of localized orbitals and their orientation. In addition, minimization with respect to the number of localized orbitals yields valency which is defined as an integer number of electrons available for band formation,  $N_{\text{val}} = Z - N_{\text{core}} - N_{\text{SIC}}$ , where  $Z$  is the atomic number,  $N_{\text{core}}$  is the number of core (and semi-core) states, and  $N_{\text{SIC}}$  the number of self-interaction corrected (localized) states. Furthermore, in the SIC-LSD the occupation of each localized orbital is

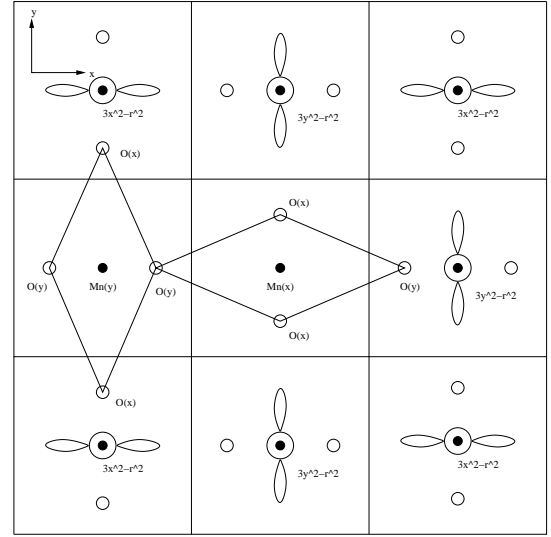


FIG. 1: Simplified view of the manganese oxygen plane in  $\text{LaMnO}_3$ . The small black circles represent the manganese atoms, while the open circles mark the positions of the oxygens. The distortion has been exaggerated to show clearly that the manganese oxygen bonds alternate between long and short in the x and y directions (designated Mn(x) and Mn(y) respectively), which is associated with the antiferro OO of the  $d_{3x^2-r^2}$  and  $d_{3y^2-r^2}$  orbitals.

determined self-consistently. When localizing an  $e_g$  orbital its symmetry is automatically broken leading to a nonzero value for the local orbital order. For example if the orbital that is localized corresponds to  $d_{3z^2-r^2}$  then the occupation of this orbital and its partner,  $d_{x^2-y^2}$ , will be different. This difference, because of hybridization effects, will not be equal to unity as it would be in a fully localized picture.

The SIC-LSD provides the quantitative comparison of all energies for  $\text{LaMnO}_3$ . This material has a distorted cubic structure with OO as shown in Fig. 1 and is an A-type antiferromagnet (A-AFM) such that the moments in the x-y planes shown in Fig. 1 are ordered ferromagnetically and the planes are stacked antiferromagnetically

TABLE I: Summary of all energy scales in  $\text{LaMnO}_3$ .

Quantity	Energy gain (m Ry per formula unit)
Electronic energy gain due to the distortion	40
Localisation energy	20
Purely electronic contribution to the orbital ordering energy	5
Relative stability of the A type antiferromagnetic state compared with ferromagnetic	1

along the c axis. Although the dominant distortion about a Mn site is tetragonal there are other components so that the net symmetry is lower. We have established that the relevant energies are: change in the total energy due to the distortion, localization energy, the purely electronic contribution to the orbital ordering energy (i.e., the change in the electronic energy induced by OO in the absence of distortion), and the magnetic ordering energy; these energy scales are summarized in Table I.

The largest electronic energy is that due to the distortion i.e., the gain in energy by imposing OO in the distorted crystal structure. The second largest energy in the problem is the localization energy which is the difference between the energies of localized and delocalized  $e_g$  states. The value is about 20 m Ry per formula unit, depending slightly on the state of magnetisation and distortion. The magnetisation comes last, as the smallest energy scale, behind the purely electronic contribution to the orbital ordering energy. The oxygen displacements around site Mn(x) are such that the site symmetry has a large,  $2_{xx} \quad yy \quad zz$ , distortion, as well as other smaller distortions that break the symmetry between y and z. The Mn(y) site has a similar distortion. Table II contains all SIC-LSD energies when a given  $e_g$  orbital has been localized on a given site, for A-AFM spin ordering. All calculations were done for the experimental distorted structure.[9]

The following points may be seen from this table. First, the most favourable state is the antiferro orbital ordering (AFOO) on the correct site coupled with antiferromagnetic spin ordering as observed experimentally. Second, the results for scenarios 6 and 7 should be identical from symmetry. They were calculated independently and the difference between them represents an estimate of the error on our calculations; the same is true for scenarios 9 and 10. Third, the size of the total electronic energy favouring the orbital ordering is found from the most and least favorable AF scenarios 1 and 4, which differ by 78 m Ry, half of which is then the energy gain due to OO, i.e. the largest energy scale of Table I. More explicitly, the states in scenarios 1 and 3 have identical

TABLE II: Results for several scenarios where the three  $t_{2g}$  orbitals and an additional  $e_g$  state are localized on the manganese atoms in fully distorted A-AFM structure of  $\text{LaMnO}_3$ . The first column gives the numbering of the scenarios which involve AFOO and ferro (F) OO. Columns 2 and 3 indicate which  $e_g$  orbital is localized on the manganese atoms with the long manganese-oxygen bonds in the x and y directions respectively. The relative energies  $E$ , with respect to the ground state with the localized  $d_{3x^2-r^2}$  orbital on the Mn(x) sites and the  $d_{3y^2-r^2}$  state on the Mn(y) atoms, is displayed in column 4 (A-AFM). Column 5 refers to relative energies  $E_d$  obtained from a localized model which incorporates only the orbital ordering in a purely tetragonal distortion. (see text)

	#	Mn(x)	Mn(y)	A-AFM	
				$E$ (m Ry)	$E_d$ (m Ry)
AFOO	1	$d_{3x^2-r^2}$	$d_{3y^2-r^2}$	0	0
	2	$d_{z^2-x^2}$	$d_{y^2-z^2}$	8.5	20
	3	$d_{3y^2-r^2}$	$d_{3x^2-r^2}$	65.2	59
	4	$d_{y^2-z^2}$	$d_{z^2-x^2}$	78.1	78
FOO	5	$d_{x^2-y^2}$	$d_{x^2-y^2}$	27.2	20
	6	$d_{3x^2-r^2}$	$d_{3x^2-r^2}$	39.7	29
	7	$d_{3y^2-r^2}$	$d_{3y^2-r^2}$	40.5	29
	8	$d_{3z^2-r^2}$	$d_{3z^2-r^2}$	49.5	59
	9	$d_{z^2-x^2}$	$d_{z^2-x^2}$	56.6	49
	10	$d_{y^2-z^2}$	$d_{y^2-z^2}$	57.3	49

pattern of antiferro orbits. The difference between them is that in the former case the lobes of the orbit match the lattice distortion, while in the latter case the orbit is misaligned with respect to the distortion. Band structure effects favour these states equally and the difference in their energies represents the importance of the lattice distortion for the OO energy.

The energy scale that characterises the stability of A-AFM versus FM is the smallest energy scale, at 1 m Ry, which is similar to energies that gave correct exchange constants for NiO (100) surface.[10] Thus, the ordering sequence of the rows will be the same for the A-AFM and the FM structures, which indicates that the dominant cause of the orbital ordering is not the A-AFM magnetic structure, as has been postulated.[11, 12]

It is instructive to see how far a localized model that assumes only a locally pure tetragonal distortion can account for the ab initio results. The energy per site is given by  $u = u_0 - u_D \cos 2\phi$  where  $u_0$  and  $u_D$  are the energies that do not and do depend on the distortion respectively. The angle  $\phi$  defines the orbit. For the site Mn(x) we have  $\phi = 0 : d_{3x^2-r^2}$ ,  $\phi = 60^\circ : d_{x^2-y^2}; d_{x^2-z^2}$ ,  $\phi = 120^\circ : d_{3y^2-r^2}; d_{3z^2-r^2}$ ,  $\phi = 180^\circ : d_{y^2-z^2}$ , and equivalently for the Mn(y) site. The energies of scenarios 1 and 4 may be used to  $u_0 - u_D = 39$  m Ry for the A-AFM phase. The results given in column 5 of Table II are found using this expression. It is seen that the order of energies obtained by this simple model repro-

duces the trends seen in the ab initio results. Moreover, most ab initio energies lie within 10 mRy of this very simple model. It appears that the discrepancy between the model and the first principles results is mostly due to other distortions than tetragonal. In order to investigate this we have performed ab initio calculations for a crystal with a pure tetragonal distortion (of the observed magnitude). In this case we found a slightly increased value for  $u_D$  (42 mRy) and the deviations between the model and the first principles calculation are reduced to 5 mRy, for all scenarios. The size of these remnant energy fluctuations designates the scale of the band electrons' contribution to the total energy. The imposed O-O, lattice distortion and magnetic structure induce changes to the conduction electron states, which leads to changes of the order of 5 mRy to the total energy. This represents the third energy scale of Table I, which is the second smallest of the energy scales considered. Another estimate for the band-electronic effects was obtained by evaluating the O-O total energy variations in the cubic phase. Our calculations gave 3.7 and 8.3 mRy in this case, for FM and A-AFM ordering respectively, i.e. O-O is drastically suppressed without the lattice distortion.

To proceed with the analysis of the energetics of O-O in the manganites, we now consider the lattice distortion mode. The strength of the orbital-lattice interaction may be deduced from the measured values of the elastic constants and the size of the lattice distortion. To see this, we follow Ref. 13 and consider an expansion of the total energy of an electronic system at  $T = 0$  in terms of a local distortion in the unit cell at  $R_i$ . The restoring force for that mode is characterized by the force constant  $K_i$ , and the elastic energy of the distortion has a simple harmonic dependence on amplitude. Countering this is the nonzero orbital order, which contributes a negative energy:

$$\begin{aligned} U_{\text{tot}} &= U_0 + U_{\text{el}}(f_{\text{ig}}) + \frac{1}{2} \sum_i K_i (u_i)^2 \\ &= U_0 + U_{\text{el}}(0) + \sum_i U_{\text{el}}(f_{\text{ig}}) + \frac{1}{2} \sum_i K_i (u_i)^2: \quad (1) \end{aligned}$$

In deriving this expression we assumed that only linear terms in  $u_i$  were required for the O-O energy, and defined

$$u_i = \frac{\partial U_{\text{el}}(f_{\text{ig}})}{\partial u_i}:$$

At equilibrium, the elastic and O-O energies must balance, and the distortion parameter is found by minimizing the energy, i.e.,  $u_i = \frac{u_i}{K_i}$ . Therefore the total lowering of energy due to the lattice distortion and O-O is found by substituting the above expression for  $u_i$  into equation (1):

$$U = U_{\text{el}}(0) + \frac{1}{2} \sum_i K_i (u_i)^2 = U_{\text{el}}(0) + \frac{1}{2} \sum_i u_i^2:$$

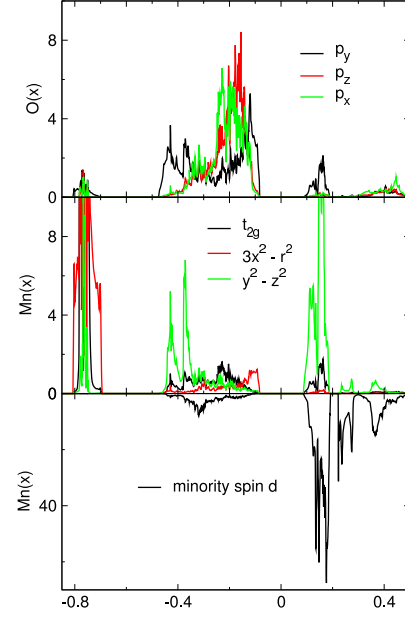


FIG. 2: The orbital and spin resolved densities of states corresponding to scenario 1 (see Table II), i.e. with the  $e_g$  lobes oriented along the long Mn-O bonds. The top panel shows the majority spin partial p densities of states for the O(x) sites, while the middle and lower panels show the majority and minority (summed over all d orbitals) spin partial d densities of states for the Mn(x) site respectively. The energies (in Ry) are relative to the Fermi energy at  $E = 0$ . The partial densities of states are in units of states/spin/Ry.

The distortions are known in the manganites,  $u_i \approx 0.30$  Å, [9] as are also the optic phonon frequencies, leading to  $K \approx 12.5$  eV/Å<sup>2</sup>, [13]. Hence, we can determine an experimental value of  $u_i = 3.5$  eV/Å. The SIC-LSD theory leads to the estimate  $u_i = u_D = u_i \approx 1.8$  eV/Å, which is to be considered in excellent agreement, given the general uncertainty, not least in estimating the appropriate value of  $K$ . [13] Otherwise stated, neglecting  $U_{\text{el}}(0)$ , a total Jahn-Teller ordering energy of  $\frac{1}{2}u_D \approx 20$  mRy is arrived at, which is in rather good agreement with the estimate of 0.48 to 0.58 eV = 35 to 43 mRy of Ref. 13.

To shed more light on the hybridization effects involved in O-O, we inspect in detail the magnetic and orbital quantum numbers resolved densities of states for two O-O configurations, namely scenarios 1 and 3 of Table II which are shown in Figs. 2 and 3 respectively. Localised orbitals are seen to have only marginal admixture (below 0.1 electron) of the delocalized  $e_g$  state. The latter (in green) can be found both in the valence and conduction bands. The localized orbitals do still contribute some weight in the valence and conduction bands of the Mn(x) majority DOS in Figs. 2 and 3. In particular,  $t_{2g}$  states contribute to the valence and conduction bands. This reflects the slight hybridization of the  $t_{2g}$  states, showing that they are not of pure ionic character but acquire

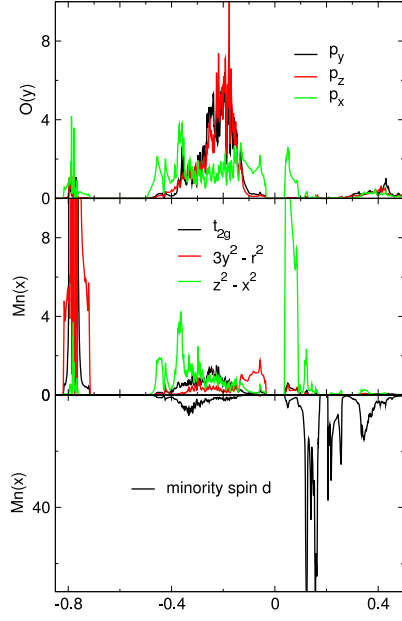


FIG. 3: The same as Fig. 2 but for scenario 3 (see Table II), i.e., the  $e_g$  lobes are oriented along the short Mn-O bonds. The top panel shows the majority spin partial p densities of states for the O(y) sites.

some covalency. For the localized  $e_g$  state this hybridization increases and is most pronounced for  $d_{3y^2-r^2}$  in Fig. 3. Here we find  $d_{3y^2-r^2}$  states in both the conduction band and at the top of the valence band, summing up to 0.2 electrons. Obviously, this localized state, whose lobes point along the short Mn-O bond length, hybridizes strongly with the  $p_x$  orbital of O(y) site and this can be seen as the  $p_x$  weight in the conduction band of O(y) partial DOS in Fig. 3. In contrast the  $d_{3x^2-r^2}$  weight in the valence and conduction bands for scenario 1 is less than the  $d_{3y^2-r^2}$  weight in scenario 3. In scenario 1 the  $e_g$  orbital is more localized: 0.82 localized  $d_{3x^2-r^2}$  electrons versus 0.74  $d_{3y^2-r^2}$  in the DOS peak around -0.8 Ry.

These results can be easily understood in terms of the OO reducing the overlap between the localized (SIC)  $e_g$  states and the 2p states of the adjacent oxygen atoms. This is reflected in the DOS of scenario 3 by the increased hybridization in the O 2p channel around -0.8 Ry, over the whole width of the valence band and even in the conduction band (Fig. 3), in comparison with the DOS of scenario 1. Thus localized  $e_g$  states which have lobes along the long manganese oxygen bonds will be energetically favourable configurations, while those that point along the short manganese oxygen bonds will correspond to energetically unfavourable configurations. Therefore the next two in the sequence of favourable scenarios are also antiferro OO involving in one case  $d_{z^2-x^2}$  and  $d_{y^2-z^2}$

(8.5 m Ry above the ground state) and in the other case the  $d_{3x^2-r^2}$  and  $d_{3y^2-r^2}$  but with ferromagnetic spin arrangement (unfavourable by 1 m Ry). It is significant that even with the ferromagnetic spin arrangement the antiferro OO is lowest in energy indicating again the importance of the JT effect.

In summary, using the SIC-LSD theory it has been possible to investigate the orbital, spin and charge ordering of distorted  $\text{LaMnO}_3$ . We find that our calculated values for the orbital energy depend strongly on the lattice distortion and are essentially independent of the magnetic order. We have used various numerical estimates to support our claim that the Jahn Teller interaction is the dominant effect in producing OO. The lattice effects are big enough to account for the observed OO, meaning that it is not necessary to invoke additional contributions of an electronic origin. This, however, should be compared with the results of other papers, [11, 12] where it is claimed that OO could occur from electronic effects alone. We agree with this in so far that we also find an electronic effect of the correct symmetry. However, we find that the energy associated with the pure electronic effect is relatively small and that the size of the effect associated with the distortion is large enough to give rise to the structural transition. In addition, this could be corroborated by comparing with independent experiments. This is an important finding for the transport in the doped materials because as the electrons become delocalised the lattice is unable to respond fast enough and one reaches the large polaron regime. On the other hand OO that is purely electronic could coexist in the metallic phase giving rise to residual OO and extra contributions to the scattering.

- 
- [1] Caciuro, R., et al, Phys. Rev. B 65, 174425 (2002).
  - [2] Shiina, R., et al, Physica B 312, 696 (2002).
  - [3] Coey, J.M.D., et al, Adv. Phys. 48, 167 (1999).
  - [4] Goodenough, J.B., Phys. Rev. 100, 564 (1955).
  - [5] Perdew, J.P. and Zunger, A., Phys. Rev. B 23, 5048 (1981).
  - [6] Temmerman, W.M. et al. in Electronic Density Functional Theory: Recent Progress and New Directions, edited by J.F. Dobson et al., (Plenum, New York, 1998).
  - [7] Strange, P. et al, Nature 399, 756 (1999).
  - [8] Temmerman, W.M. et al, Phys. Rev. Lett. 86, 2435 (2001).
  - [9] Elmers, J.B.A.A. et al, J. Solid State Chem. 3, 238 (1971).
  - [10] D.K. Odieritzsch et al, Phys. Rev. B 66, 064434 (2002).
  - [11] Medvedeva, J.E. et al, Phys. Rev. B 65, 172413 (2002).
  - [12] Okamoto, S. et al, Phys. Rev. B 65, 144403 (2002).
  - [13] Millis, A.J., Phys. Rev. B 53, 8434 (1996).